Solvothermal Reduction of Chemically Exfoliated Graphene Sheets

Hailiang Wang, Joshua Tucker Robinson, Xiaolin Li, and Hongjie Dai*

Department of Chemistry and Laboratory for Advanced Materials, Stanford University, Stanford, California 94305

Received May 26, 2009; E-mail: hdai@stanford.edu

Graphene has attracted much attention because of its interesting properties and potential applications.[1−3] Chemical exfoliation methods for making graphene have recently been developed[4,5] for use in large-scale assembly[6] and applications such as composites[7] and Li ion batteries.[8] Although these chemical exfoliation methods are efficient, they involve oxidation of graphene and introduce defects in the as-made sheets. Hydrazine reduction at temperatures below 100 °C has been shown to partially restore the structure and conductance of graphite oxide (GO).[4,9−11] However, the reduced GO still shows strong defect peaks in Raman spectra and has a resistivity higher than that of pristine graphene by 2−3 orders of magnitude.[4,9−11] It is important to produce much less defective graphene sheets (GS) than GO and develop more effective graphene reduction.

Recently, we reported a mild exfoliation−reintercalation−expansion method for forming high-quality GS with higher conductivity and a lower degree of oxidation than GO.[5] Here we present a 180 °C solvothermal reduction method for our GS and GO. The solvothermal reduction is more effective than the earlier reduction methods in lowering the oxygen and defect levels in GS, increasing the graphene domains, and bringing the conductivity of GS close to that of pristine graphene. The reduced GS possess the highest degree of pristinity among chemically derived graphene.

GS were made from natural graphite flakes, intercalated by oleum and tetrabutylammonium cations, and suspended in N,N-dimethylformamide (DMF) [see the Supporting Information (SI)].[5,6] Solvothermal reduction was carried out in DMF at 180 °C using hydrazine monohydrate as the reducing agent (see the SI). The GS (average size ≈ 300 nm on the side) remained well-dispersed in DMF after reduction. The homogeneous suspension contained mostly single sheets, as observed by atomic force microscopy (AFM) on SiO$_2$ (Figure 1). The apparent height of the GS was ∼0.8−1.0 nm (Figure S1 in the SI), suggesting single-layer GS.

We also reduced our GS at room temperature and 80 °C with hydrazine monohydrate. After these reductions, the Raman D/G intensity ratios (where the D peak is a defect peak due to intervalley scattering[12] and G refers to the graphene G peak) were higher than for the as-made GS (Figure 2a,b), indicating an increase in the number of smaller graphene domains. This is usually observed in the Raman spectra of reduced GO.[4,10,11] In contrast, when our GS were reduced under solvothermal conditions (180 °C), the reduced GS showed an average D/G intensity ratio lower than that of the as-made GS (Figure 2a,b). Since the Raman D/G intensity ratio is proportional to the average size of the sp^2 domains,[4,12] the solvothermal reduction actually increased the average size of the crystalline graphene domains in our GS, which has been unattainable by solution-phase reduction of GO.

We observed that the D′/G (Figure 2c) and S3/2D (Figure S4a,b) intensity ratios (where the D′ peak is a defect peak due to intravalley scattering,[12] the S3 peak is a second-order peak due to the D−G combination, and 2D refers to the graphene 2D peak) of the GS also decreased significantly after solvothermal reduction, suggesting that the defect concentration in the GS was much reduced. This was
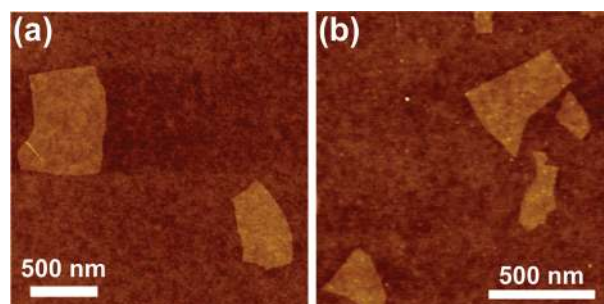

Figure 1. AFM images of (a) as-made and (b) solvothermally reduced GS.
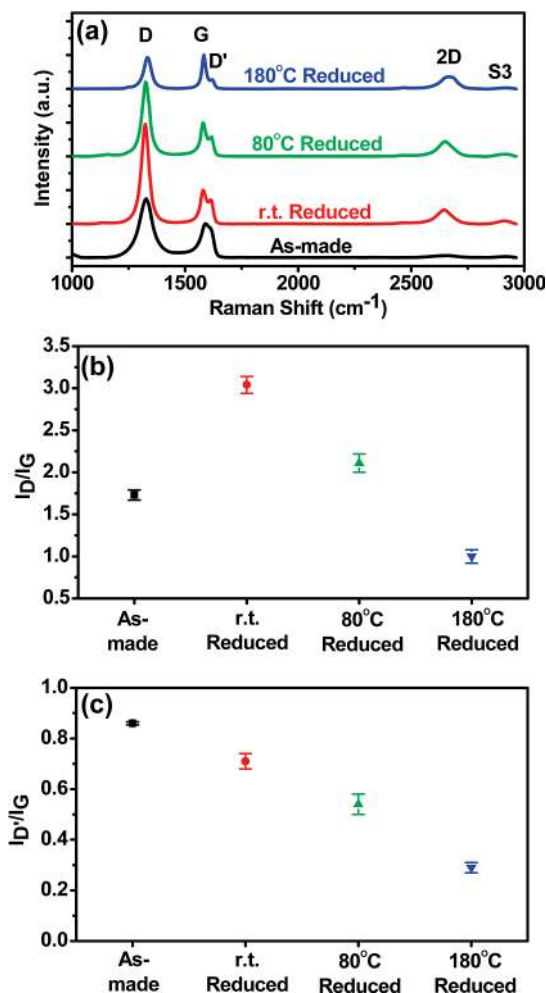

Figure 2. Raman characteristics of as-made and different types of reduced GS film samples: (a) Raman spectra; (b) D/G intensity ratios; (c) D′/G intensity ratios. Error bars are based on Raman spectra taken at 5−10 different spots on each sample.

accompanied by a lower oxygen content in the solvothermally reduced GS compared to the as-made GS sample, as revealed by Auger elemental analysis (Figure S6a, Table S2). Although the trend of I_D/I_G was not monotonic with respect to reduction temperature (Figure 2b), the I_D/I_G (Figure 2c) and I_{S3}/I_{2D} (Figure S2) ratios decreased monotonically with increasing reduction temperature. These data suggest that solvothermal reduction of GS is effective with respect to both oxygen content and defect density.
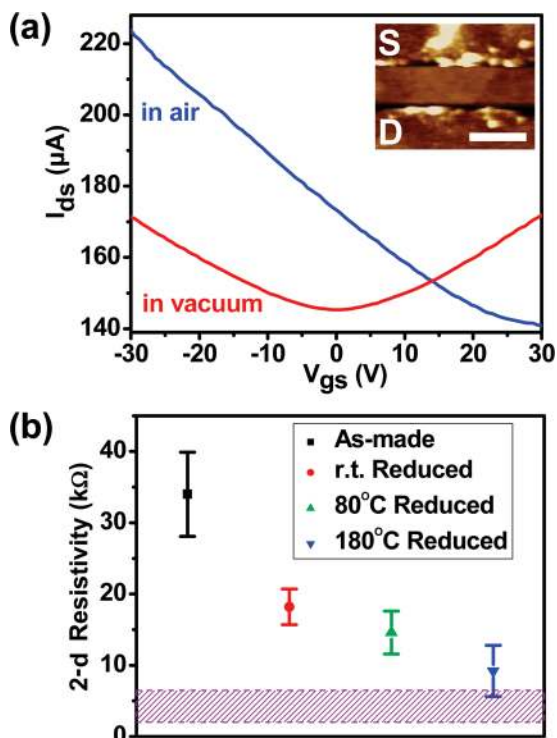

Figure 3. Electrical transport characteristics of solvothermally reduced GS. (a) Current−gate voltage (I_{ds}−V_{gs}) curves for a device measured in air (blue curve) and in vacuum after high-current cleaning (red curve). The inset shows an AFM image (scale bar: 200 nm) of single GS-bridging source (S) and drain (D) electrodes on 100 nm SiO_2 on p^{2+}-Si, which was used as a back-gate. (b) Resistivity of as-made and different types of reduced GS. The purple region shows the resistivity range of pristine graphene reported in refs 13−15.

Electrical devices were fabricated (see the SI) with the as-made and reduced GS. With the increase in reduction temperature, the average two-dimensional (2-D) resistivity (defined as RW/L, where R is the resistance of the device and W and L are the GS width and channel length, respectively) of the GS decreased (Figure 3b) after solvothermal reduction reached a minimum of less than 10 kΩ, which is close to that of pristine peel-off graphene sheets.[13−15] The current−bias (I_{ds}−V_{ds}) curves for the solvothermally reduced GS were linear (Figure S8), as expected for high-quality graphene but not GO. Intrinsic Dirac-like behavior of our solvothermally reduced GS (Figure 3a) was always observed after removal of absorbed molecules by high-current electrical annealing[6,16] in vacuum (see the SI, Figure S7).

Reduction was also carried out for GO made by a modified Hummers method (see the SI).[17] As revealed by Raman and electrical measurements, the solvothermally reduced GO had a higher quality than GO reduced at lower temperatures. However, unlike the decrease in the D/G intensity ratio of GS with increasing reduction temperature, a monotonic increase of the D/G intensity ratio of GO with increasing reduction temperature was observed (Figure S3a,b), indicating that large numbers of small sp^2 domains

exist in GO even after solvothermal reduction. The solvothermally reduced GO showed much broader Raman peaks than the reduced GS, suggesting much more remaining disorder in GO originating from harsh oxidation (see Figure S5 and Table S1)[12] with a high oxygen content, as shown by Auger elemental analysis (Figure S6b, Table S2). The average 2-D resistivity of solvothermally reduced GO was still more than 100 times higher than that of solvothermally reduced GS (Figure S9c). The I_{ds}−V_{ds} curves of solvothermally reduced GO showed clear nonlinear exponential characteristics (Figure S9b), that were well-fitted with the 2-D variable-range hopping model,[18] suggesting the existence of considerable defect regions between graphene domains. Thus, although our solvothermal reduction is more effective than those under previous conditions, large numbers of defects still exist in GO that are difficult to reduce, limiting the size of the sp^2 domains in the reduced GO.

The improved effectiveness of our solvothermal reduction could be due to more thorough removal of oxygen functional groups by hydrazine at high temperature, which was corroborated by the low oxygen content and decreased "solubility" of the reduced GS. The solvothermal condition could also help to anneal structural defects in the GS. However, more work is still needed in order to reveal the detailed reduction mechanism and pathways.

In conclusion, we have developed an effective solvothermal reduction method to decrease the number of defects and the oxygen content in graphene sheets and GO. We have succeeded in decreasing the resistivity of chemically derived graphene to a value approaching that of pristine graphene with the solution-phase reduction method. The resulting high-quality GS could be useful in various types of basic and applied research on graphene materials.

Supporting Information Available: Experimental details and additional AFM, Raman spectroscopy, Auger spectroscopy, and electrical device characterizations. This material is available free of charge via the Internet at http://pubs.acs.org.

References

(1) Novoselov, K. S.; Geim, A. K.; Morozov, S. V.; Jiang, D.; Zhang, Y.; Dubonos, S. V.; Grigorieva, I. V.; Firsov, A. A. *Science* **2004**, *306*, 666–669.
(2) Li, X.; Wang, X.; Zhang, L.; Lee, S.; Dai, H. *Science* **2008**, *319*, 1229–1232.
(3) Jiao, L.; Zhang, L.; Wang, X.; Diankov, G.; Dai, H. *Nature* **2009**, *458*, 877–880.
(4) Stankovich, S.; Dikin, D. A.; Piner, R. D.; Kohlhaas, K. A.; Kleinhammes, A.; Jia, Y.; Wu, Y.; Nguyen, S. T.; Ruoff, R. S. *Carbon* **2007**, *45*, 1558–1565.
(5) Li, X.; Zhang, G.; Bai, X.; Sun, X.; Wang, X.; Wang, E.; Dai, H. *Nat. Nanotechnol.* **2008**, *3*, 538–542.
(6) Wang, H.; Wang, X.; Li, X.; Dai, H. *Nano Res.* **2009**, *2*, 336–342.
(7) Eda, G.; Chhowalla, M. *Nano Lett.* **2009**, *9*, 814–818.
(8) Yoo, E. J.; Kim, J.; Hosono, E.; Zhou, H.; Kudo, T.; Honma, I. *Nano Lett.* **2008**, *8*, 2277–2282.
(9) Eda, G.; Fanchini, G.; Chhowalla, M. *Nat. Nanotechnol.* **2008**, *3*, 270–274.
(10) Park, S.; An, J.; Jung, I.; Piner, R. D.; An, S. J.; Li, X.; Velamakanni, A.; Ruoff, R. S. *Nano Lett.* **2009**, *9*, 1593–1597.
(11) Luo, Z.; Lu, Y.; Somers, L. A.; Johnson, A. T. C. *J. Am. Chem. Soc.* **2009**, *131*, 898–899.
(12) Ferrari, A. C. *Solid State Commun.* **2007**, *143*, 47–57.
(13) Dan, Y.; Lu, Y.; Kybert, N. J.; Luo, Z.; Johnson, A. T. C. *Nano Lett.* **2009**, *9*, 1472–1475.
(14) Reina, A.; Jia, X.; Ho, J.; Nezich, D.; Son, H.; Bulovic, V.; Dresselhaus, M. S.; Kong, J. *Nano Lett.* **2009**, *9*, 30–35.
(15) Farmer, D. B.; Golizadeh-Mojarad, R.; Perebeinos, V.; Lin, Y.; Tulevski, G. S.; Tsang, J. C.; Avouris, P. *Nano Lett.* **2009**, *9*, 388–392.
(16) Wang, X.; Li, X.; Zhang, L.; Yoon, Y.; Weber, P. K.; Wang, H.; Guo, J.; Dai, H. *Science* **2009**, *324*, 768–771.
(17) Hummers, W. S., Jr.; Offeman, R. E. *J. Am. Chem. Soc.* **1958**, *80*, 1339.
(18) Kaiser, A. B.; Gómez-Navarro, C.; Sundaram, R. S.; Burghard, M.; Kern, K. *Nano Lett.* **2009**, *9*, 1787–1792.

JA904251P